Synthesis and Characterization of Phase Change Microcapsules Containing Nano-Graphite

Yeng-Fong Shih[*], Hong-Hao Chen

Department of Applied Chemistry, Chaoyang University of Technology, Taichung, Taiwan, ROC

Abstract

This study uses the sol-gel method to modify the phase change microcapsules. The phase change material (PCM) is encapsulated by a polymer shell to reduce the leakage in the solid-liquid transition. Furthermore, the nano-graphite particle (NGP) is introduced into the shell to increase its thermal conductivity. The particle size and enthalpy value of the obtained microcapsules are approximately 3 μm and 150.3 J/g, respectively. The results show that the encapsulation efficiency of PCM in the prepared microcapsules is increased and the crystallization rate of PCM becomes faster when the NGP is added. The obtained microcapsules and wood flour are incorporated into high-density polyethylene (HDPE) to form a wood-plastic composite (WPC). The results indicate that the tensile and impact strengths of the WPC are 24.1 MPa and 48.7 J/m, respectively. Moreover, it is observed that the addition of these phase-change microcapsules can improve the heat dissipation of HDPE and accelerate the speed of thermal diffusion.

Keywords: microcapsules, phase change materials, sol-gel method, nano-graphite, polymer composite material

1. Introduction

The rapid development of industrial technology has brought about a convenient living standard, but it has also incurred a shortage of electricity and rapid consumption of natural energy, environmental pollution, and greenhouse gas. Given that sources of energy such as petroleum and coal are non-renewable and have environmental concerns, energy-saving, and storage materials are of great significance to sustainable development. Thermal energy storage is divided into sensible heat, latent heat, and chemical energy storage [1-4]. Among them, phase change material (PCM) attracts attention owing to the function of latent heat storage [5-7]. During the phase change process, it absorbs and releases a large amount of heat energy, while its temperature remains unchanged. PCMs are considerably applied in heat storage and have the advantages of high energy storage density, small volume change, and small temperature change [8-11].

Among the four types of PCMs (solid-solid, solid-liquid, solid-gas, and liquid-gas), the solid-liquid type is the most widely used. Concerning the chemical structure, PCMs can be classified into inorganic and organic categories. Organic PCMs including substances like fatty acids, octadecane, paraffin, and polyethylene glycol (PEG) [12] have been pervasively employed in solar energy utilization, air conditioning, photovoltaic, textile, and building energy saving [13-14]. Meanwhile, PCMs are also extensively deployed in buildings for thermal storage, reducing energy consumption in air conditioning, enhancing thermal comfort, and improving building durability. According to IEA/SHC Task 42 (ECES Annex 29) on Compact Thermal Energy Storage, PCMs are crucial to the advancement of building efficiency and ensuring thermal comfort [15].

---

* Corresponding author. E-mail address: z0903590036@gmail.com

However, PCMs are susceptible to cause problems such as leakage or pollution of the environment when melted [16-18], which incurs limitations. Therefore, microencapsulated phase change material (MEPCM) with a core/shell structure has been developed to prevent the leakage of melted PCM during phase change [19-20]. Moreover, the thermal conductivity of most materials is generally low and remains to be a challenge, as it results in a slow rate of latent heat transfer. Thus, many researchers have incorporated carbon fiber [21], carbon nanotube (CNT) [22], graphite [23], metal [24], or metal oxide [25] to improve the thermal conductivity of MEPCM.

This study is to prepare the microcapsules by a sol-gel method [26], and the PCM is encapsulated with a copolymer shell to reduce leakage during the solid-liquid transition. In addition, nano-graphite particles (NGP) are added to the shell to increase its thermal conductivity.

(1) Firstly, Methyl methacrylate (MMA) and triethoxyvinylsilane (TEVS) are copolymerized into a prepolymer, and the purpose of adding TEVS is to improve the compatibility between the shell layer and the graphite heat-conducting material.

(2) Subsequently, the prepolymer is added to the solution prepared by polyvinyl alcohol (PVA), octadecane, and tetraethoxysilane, using ethylene glycol dimethacrylate (EGDMA) as a bridging agent.

(3) Finally, the nanometer with high thermal conductivity NGP is added to obtain the thermally conductive phase-change microcapsules containing nano-graphite in the shell and octadecane in the core.

Consequently, these microcapsules can provide a temperature-regulating effect and improve the rate of heat transfer compared to traditional ones. Furthermore, these MEPCMs will be integrated into wood-plastic composites (WPC) to create building materials with a thermal storage effect, ultimately reducing the need for air conditioning.

2. Materials & Methodology

This section provides the materials and methods for preparing microcapsules, acidified NGP, NGP-containing microcapsules, and composite materials. Additionally, the analysis procedures for the materials' morphology, thermal properties, and mechanical strengths were described.

2.1. Materials

The materials were enumerated as follows: TEVS, benzoyl peroxide (BPO), and MMA supplied by Acros Organics, tetraethylorthosilicate (TEOS) was supplied by Seedchem, octadecane supplied by Alfa Aesar, and EGDMA as the crosslinking agent was supplied by Alfa Aesar. Meanwhile, all the following compounds and mixtures were of reagent grade, with no further purification upon use. PVA with m.p. of 200 °C and density of 1.19-1.31 g/cm^3 was supplied by Taiwan Chang Chun Group. NGP of density 1.8 g/cm^3 and particle size 50 nm was supplied by Conjutek Co., Taiwan. High-density polyethylene (HDPE) was supplied by Formosa Plastics Corporation, maleic anhydride grafted polyethylene (MAPE) was supplied by E.Chang Trading Co., Ltd., and wood flour (WF) was supplied by Everlast NFC Co., Ltd.

2.2. Preparation of microcapsules

First, 0.054 g of BPO, and 45 g of MMA were added to 9 g of TEVS and prepolymerized in an oil bath at 80 °C for 60 minutes under nitrogen with a rotation speed of 280 rpm to obtain copolymer. Second, an aqueous solution of 1.5 wt% PVA was prepared by dissolving 22.5 g of PVA into 1500 ml of deionized water before adding octadecane (as PCM) and TEOS. The mixture was placed in a homogenizer and mixed thoroughly at 5000 rpm for 5 minutes. Subsequently, the previously obtained copolymer was added to this homogenized mixture and mixed at 5000 rpm for another 5 minutes. Then, 4 g of EDGMA and 0.56 g of BPO were added to the mixture and reacted in an oil bath at 80 °C for 24 hours with stirring, followed by cooling, centrifugation, filtration, and drying to obtain microcapsules (denoted as MEPCM) as shown in Fig. 1.
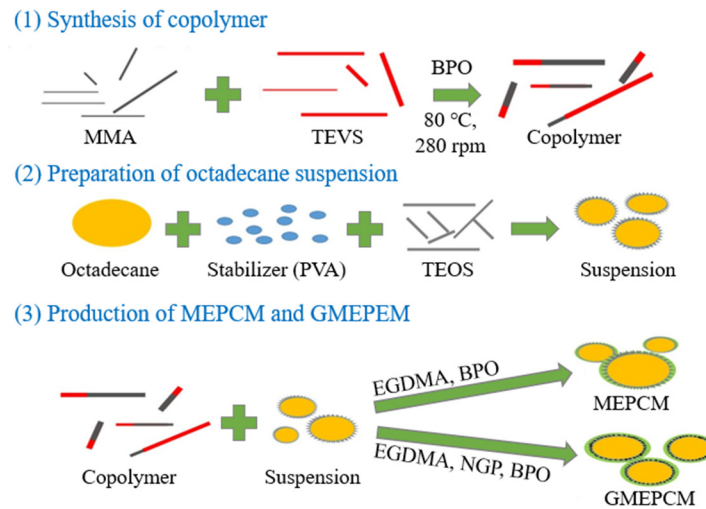
Fig. 1 Flow chart of microcapsule preparation

2.3. Preparation of acidified NGP

NGP was dried first to remove any residual moisture, then added to a solution consisting of sulfuric acid and nitric acid (3:1) while stirring at 90 °C for two hours. The resulting mixture was then transferred to an ice bath, followed by centrifugation, filtration, neutral washing, and drying to obtain acidified NGP.

2.4. Preparation of NGP-containing microcapsules

Except for the final step, the other preparation steps are similar to those of MEPCM. Finally, BPO, EDGMA, and NGP were added to the mixture and reacted in an oil bath at 80 °C for 24 h with stirring, followed by cooling, centrifugation, filtration, and drying to produce NGP-containing PCM microcapsules, denoted as GMEPCM, as depicted in Fig. 1.

2.5. Preparation of composite material

HDPE, MAPE, GMEPCM, and WF were dried in a 60 °C oven for 1 day to remove water and then melted with a mixing machine at 50 rpm and 150 °C according to different proportions in Table 1. Subsequently, the mixture was pressed at 150 °C and 60 psi, and kept for three minutes, then released the pressure for one minute. This procedure was repeated 3 times, then a series of test pieces were prepared and carried out various tests as depicted in Fig. 2.

Table 1 Formulation of composite material (wt%)

-	HDPE	MAPE	WF	GMEPCM
HD	100	-	-	-
HD-WF	80	-	20	-
HD-MA-WF	72	8	20	-
HD-GMEPCM-WF	62	8	20	10

Fig. 2 Universal testing machine

2.6. Characterization

Fourier transform infrared spectrometer (FTIR) spectra were recorded on a Spectrum Tow FTIR spectrometer using the attenuated total reflectance (ATR) method with a resolution of 2 cm^{-1} that scanned 50 times from 400 to 4000 cm^{-1} at room temperature. Before placing the sample for testing, it is necessary to scan the background value first. The subsequent steps are

placing the sample, performing sample analysis, and identifying the functional group with the same number of scans. Transmission electron microscopy (TEM; JEM-2100, JEOL, Ltd., Tokyo, Japan) was used to observe the appearance of microcapsules. The amount of heat absorbed or released during phase transitions was measured by a TA Instruments DSC Q20 differential scanning calorimeter (DSC).

Between 3-5 mg of samples were placed in an aluminum pan and the DSC at 0 °C for 5 min. It was heated from 0 to 100 °C at a heating rate of 5 °C/min, then held constant at 100 °C for 5 minutes, and then cooled to 0 °C at a cooling rate of 5 °C/min under a nitrogen atmosphere of 50 mL/min. Thermal behavior was determined using a TA Instruments TGA Q50 thermogravimetric analyzer (TGA).

The samples were scanned from 50 to 600 °C at a heating rate of 10 °C/min in the presence of nitrogen flow. It can be used to observe the composition of organic and inorganic substances in the sample. In addition to this feature, it can also determine the thermal stability, thermal degradation temperature, and char yield of the samples. First, weigh 4-6 mg of sample, place it in a TGA, analyze it in a nitrogen environment with a flow rate of 50 mL/min, raise the temperature to 50 °C, and then raise the temperature to 600 °C at a heating rate of 10 °C/min.

The universal testing machine (Fig. 2) mainly applies external force to the test piece, so that the test piece can resist the external force to reach the maximum value of its strength. The test piece is in the shape of a dumbbell, and the stretching rate is 50 mm/min. Fix the two ends of the test piece with clamps, place the distance sensor, and start stretching up and down until the test piece breaks. The thermal deformation temperature tester mainly tests the shape and size deformation of composite materials by temperature change.

Conduct a heat distortion temperature (HDT) test under 66 psi pressure, input the width and thickness of the test piece, and start the test, raise the temperature until the deformation of the test piece generates the result of 1 mm. Once the conditions are satisfied, stop the test. The impact resistance testing machine mainly uses the pendulum to break the notched test piece, and the energy absorbed by the pendulum is employed to calculate the energy consumed, and then the toughness of the material can be obtained.

The size of the test piece (Fig. 3) is about 64 mm × 13 mm × 3.2 mm rectangular test piece, which is tested after cutting a notch with the chamfering machine. The morphology of the fractured surface of a modified microcapsule containing composites was analyzed by scanning electron microscopy (SEM; JEOL JSM-6700F). The thermal conductivity analyzer uses the transient plane source (TPS) method, while the sensor is a plane probe made of a conductive metal nickel and etched to form a continuous double helix structure sheet.

During the test, the current passes through, and a certain heat source simultaneously diffusing to the samples on both sides of the probe is generated to raise the temperature. The speed of thermal diffusion depends on the heat conduction characteristics of the material, while the instrument can calculate the thermal conductivity, thermal diffusivity, and heat capacity of the material by recording the temperature and the response time of the probe.

Fig. 3 The sample for the impact test

3. Experimental Analysis

In this section, the microcapsules and NGP-containing microcapsules were compared using FTIR, TEM, DSC, and TGA analysis. Additionally, the tensile strength, impact strength, HDT, thermal conductivity, and thermal storage test of HDPED/microcapsule composites were discussed.

3.1. FTIR analysis
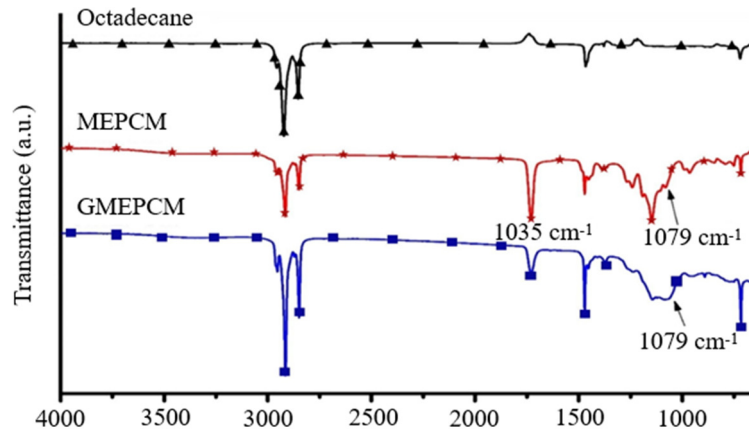
Fig. 4 FTIR spectrum of octadecane and microcapsules

In the FTIR spectrum (Fig. 4), the octadecane showed obvious characteristic peaks at 2928 cm^{-1} and 2850 cm^{-1}, which are C-H asymmetric and symmetrical stretching vibrations therein. These characteristic peaks can also be seen in MEPCM and GMEPCM. In addition, the characteristic peak at 1735 cm^{-1} of MEPCM and GMEPCM is due to the vibration of C=O in MMA. The peak intensity of MEPCM was stronger than that of GMEPCMowing to the increased content of the core and the decreased thickness of the shell after the addition of NGP, and therefore the C=O intensity decreased. This will be discussed further in the DSC analysis section. The absorption at 1079 cm^{-1} is the characteristic peak of the Si-O bond in TEVS and TEOS. The characteristic peak of GMEPCM was seemingly stronger than that of MEPCM, and it is speculated that the characteristic peak is strengthened by the bonding between TEVS and NGP. These results indicate that a copolymer composed of MMA and TEVS was synthesized, and the octadecane was successfully encapsulated in the shell of the copolymer.

3.2. Transmission electron microscopy analysis

(a) MEPCM   (b) GMEPCM
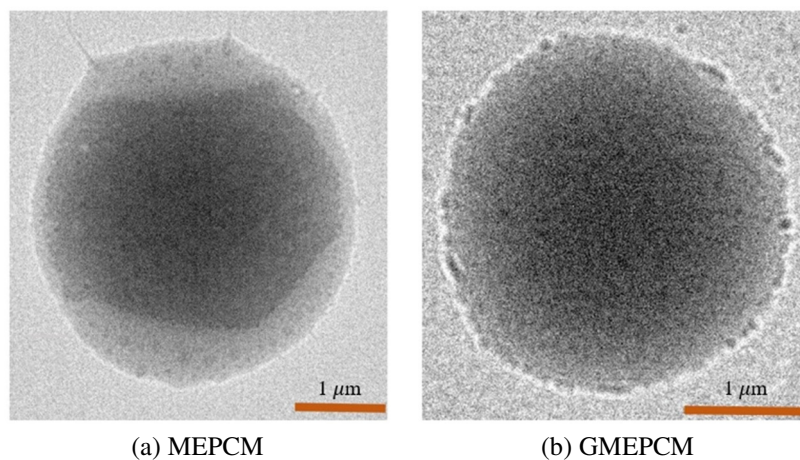
Fig. 5 Transmission electron microscopy analysis

The transmission electron microscopy analysis of MEPCM is shown in Fig. 5(a). It can be observed that the MEPCM was close to a spherical shape and the shell was transparent. The diameter of the MEPCM was about 4 μm. It revealed that the PCM can be completely encapsulated and can avoid leakage simultaneously. A spherical appearance was also found on the

microcapsule with NGP (GMEPCM) in Fig. 5(b). The diameter of the GMEPCM was about 3 μm. However, its shell did not reveal clear transparency as compared with that of MEPCM in Fig. 5(a). Such a result confirms that NGP is uniformly dispersed in the shell of GMEPCM and can also improve the thermal conductivity of the PCM.

3.3. Differential scanning calorimeter analysis

Both Fig. 6 and Table 2 show the DSC analysis of octadecane and microcapsules. From the thermograms, it can be found that the melting point of octadecane is 25.84 °C, while the melting point of MEPCM is 26.33 °C and that of GMEPCM is 28.49 °C. It can be ascribed to the mechanism of the sol-gel method that can stabilize the microcapsules and increase the thermal stability of PCM. Given such fact, the microcapsules made of polymer-coated octadecane have a higher melting point. In addition, the ΔH_m and ΔH_c of octadecane were 165.8 J/g and 160.4 J/g, MEPCM microcapsules were 109.5 J/g and 81.19 J/g, and GMEPCM microcapsules were 150.3 J/g and 139.0 J/g, respectively.
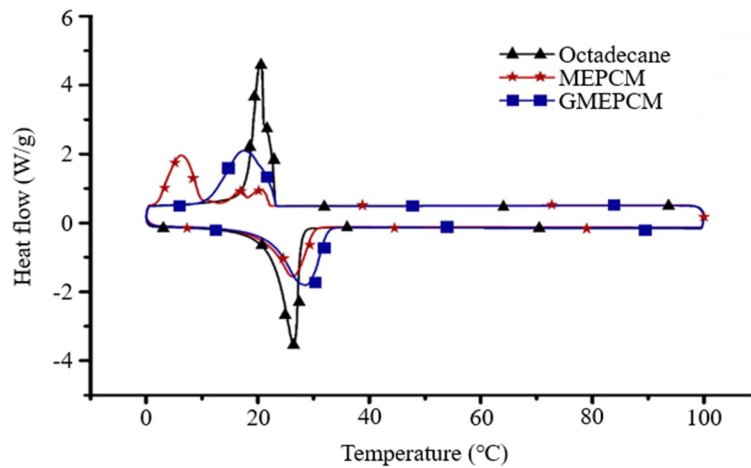
Fig. 6 DSC thermograms of octadecane and microcapsules

Table 2 DSC analysis data of octadecane and microcapsules

-	T_m (°C)	T_c (°C)	ΔH_m (J/g)	ΔH_c (J/g)	Encapsulation efficiency* (%)
Octadecane	25.84	21.40	165.8	160.4	-
MEPCM	26.33	6.70	109.5	81.19	66.04%
GMEPCM	28.49	17.63	150.3	139.0	90.65%

*$Encapsulation\ efficiency(\%) = [\Delta Hm(Microcapsule)/\Delta Hm(Octadecane)] \times 100\%$

The encapsulation efficiency (i.e., content of octadecane) of MEPCM and GMEPCM microcapsules calculated by comparing the latent heat of bulk octadecane and encapsulated octadecane is capable of elevating to 66.04 and 90.65%. The result denotes higher encapsulation efficiency of GMEPCM than that of MEPCM. Moreover, the enthalpy value of GMEPCM (150.3 J/g) stands at a greater extent than that reported in the literature (140.6 J/g) [27], indicating a robust heat storage effect. In the cooling process, the crystallization temperatures (T_c) of MEPCM and GMEPCM found were 6.70 °C and 17.63 °C, respectively. Such a result indicates the crystallization rate of MEPCM became faster with the addition of NGP owing to the fine particles of NGP being capable of acting as a nucleating agent, and the high thermal conductivity of the NGP, which promotes the crystallization of octadecane.

3.4. TGA analysis

Figs. 7-8 and Table 3 show the TGA analysis results of octadecane and microcapsules. It can be seen that merely one main degradation peak of octadecane emerged at 278.37 °C, and the char yield is 0.00% due to being an organic PCM and being completely decomposed before 600 °C. However, the two maximum degradation peaks of MEPCM stand at 261.10 °C and 386.31 °C, respectively. The former is the degradation peak of the core material in the microcapsule, and the latter is the

degradation peak of the shell layer of the microcapsule. During the preparation of MEPCM, two silanes are added to increase the thermal conductivity, and hence the maximum degradation temperature will be slightly lowered. In addition, the char yield of MEPCM increased to 1.53% due to the content of silicon elements. However, only one main degradation peak for GMEPCM emerged at 291.05 °C, and the char yield increased to 3.90% due to the increase of char yield by nano graphite, an inorganic material. Moreover, the addition of nano-graphite will improve the thermal conductivity, and the shell of GMEPCM was thin, which leads to the one main degradation peak.
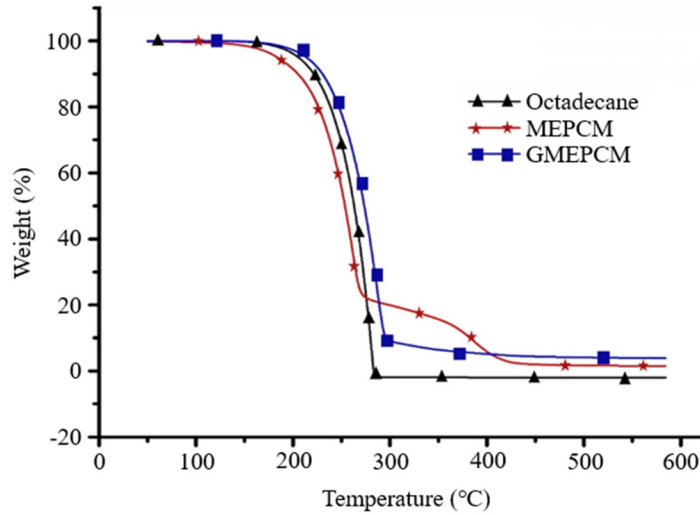
Fig. 7 TGA analysis of octadecane and microcapsules
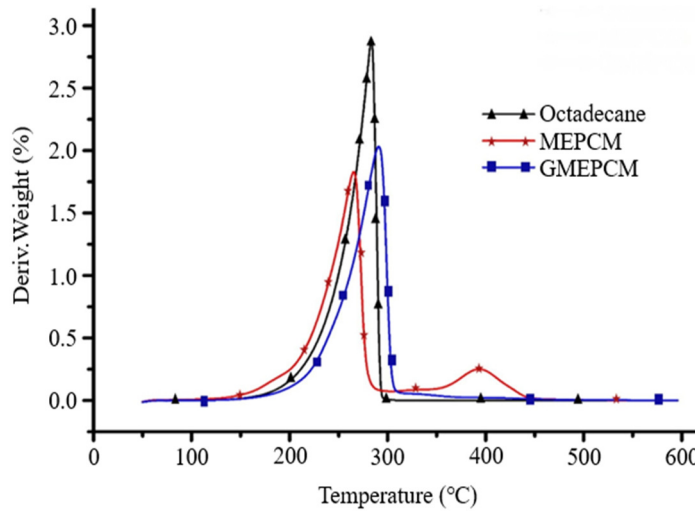
Fig. 8 DTG analysis of octadecane and microcapsules

Table 3 TGA analysis data of octadecane and microcapsules

-	Char yield (%)	T_{dmax} (°C)
Octadecane	0.00	278.37
MEPCM	1.53	261.10 386.31
GMEPCM	3.90	291.05

3.5. Tensile strength

From Fig. 9, it is observable that adding WF to HDPE (HD-WF) resulted in a decrease in tensile strength from 25.5 MPa to 19.7 MPa due to poor compatibility. Therefore, an additional compatibilizer was added to improve the compatibility to improve the strength of the composite material. The results signified that the tensile strength of HD-MA-WF has effectively increased to 30.8 MPa after adding the compatibilizer. It can be found that the tensile strength of HD-GMEPCM-WF with the

deployment of microcapsules decreased to 24.1 MPa. Meanwhile, SEM analysis reveals that GMEPCM is evenly distributed within the composite material (Fig. 10), which attests to the paucity of a significant strengthening effect on strength is unattributable to non-uniform dispersion. Instead, it should be ascribed to the absence of a reinforcing effect on the tensile strength regarding the spherical structure of GMEPCM, resulting in a slight decrease in tensile strength. Nonetheless, it is still similar to that of pure HDPE, and the composite has an additional thermal storage effect. Furthermore, Fig. 8 also illustrates that the particle size of the majority of GMEPCM is approximately 5 μm, aligning with the results of the POM analysis.
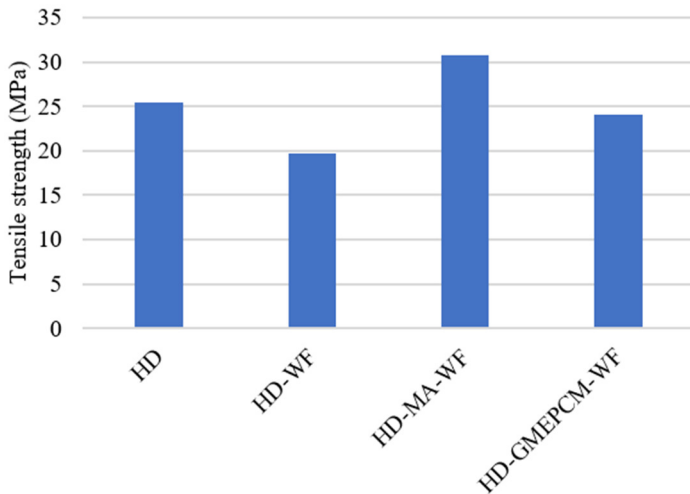
Fig. 9 Tensile strength of the materials
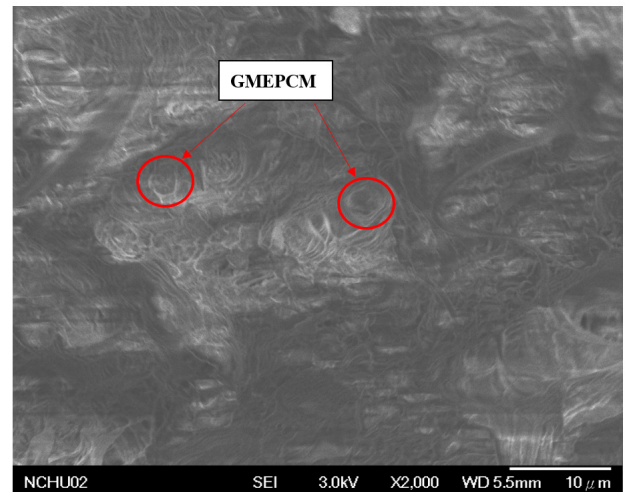
Fig. 10 SEM analysis of HD-GMEPCM-WF

3.6. Impact strength

It can be seen that the impact strength of HDPE is significantly reduced from 115.4 J/m to 51.0 J/m when adding WF to HDPE (HD-WF), as depicted in Fig. 11 since the WF is mainly used to reinforce tensile strength, and its compatibility with HDPE is poor. After adding the compatibilizer (HD-MA-WF), the impact strength increased to 53.6 J/m. It is also observable that a slight decrease in impact strength (48.7 J/m) after adding GMEPCM to HD-MA-WF (HD-GMEPCM-WF).
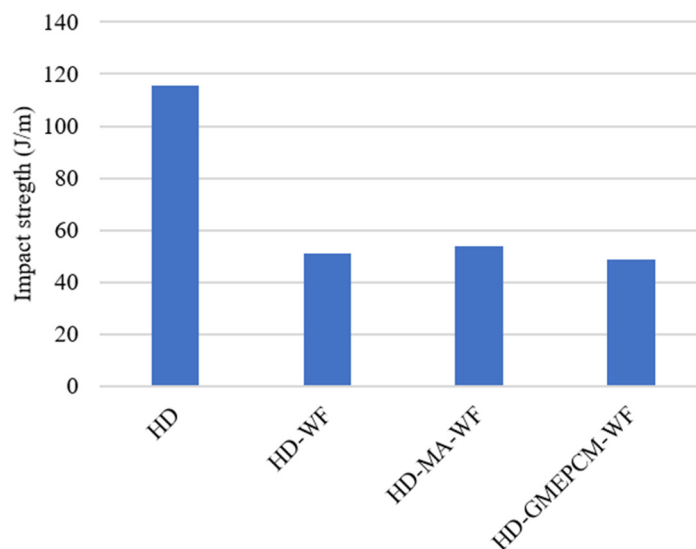
Fig. 11 Impact strength of the materials

3.7. Heat distortion temperature (HDT)

Fig. 12 exhibited that the HDT of HDPE is 87.8 °C, which increases to 102.5 °C after adding WF (HD-WF), due to the better hardness of wood fiber to resist the deformation of HDPE. The HDT of the composite further increased to 105.2 °C after adding the compatibilizer (HD-MA-WF). The result indicates that the compatibilizer is substantial to increase the interfacial

adhesion of the WF and HDPE, which subsequently improves the mechanical properties and heat resistance of the materials. In addition, the HDT of the composite material added with GMEPCM (HD-GMEPCM-WF) (95.7 °C) is larger than that of pure HDPE but lower than that of HD-MA-WFowing to the PCM being protected by the shell layer and being contained a thermally conductive material in the outer layer of the shell layer, which can improve the thermal conductivity of the material. In addition, the strength of the material decreases with the addition of microcapsules, thus reducing the heat distortion temperature.
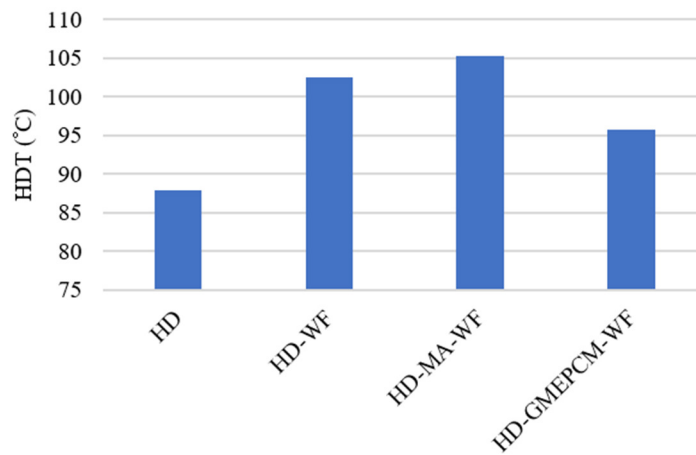
Fig. 12 Heat distortion temperature of the materials

3.8. Thermal conductivity

Fig. 13 shows the thermal conductivity of the materials. The thermal conductivity of HDPE is 0.45 W/m·K and increases to 0.50, 0.60, and 0.62 W/m·K after adding WF, compatibilizer, and GMEPCM to the composite material, respectively. It evinces that adding nano-graphite-containing microcapsules as a heat-conducting material will accelerate the rate of heat diffusion and improve the heat dissipation mechanism of HDPE.
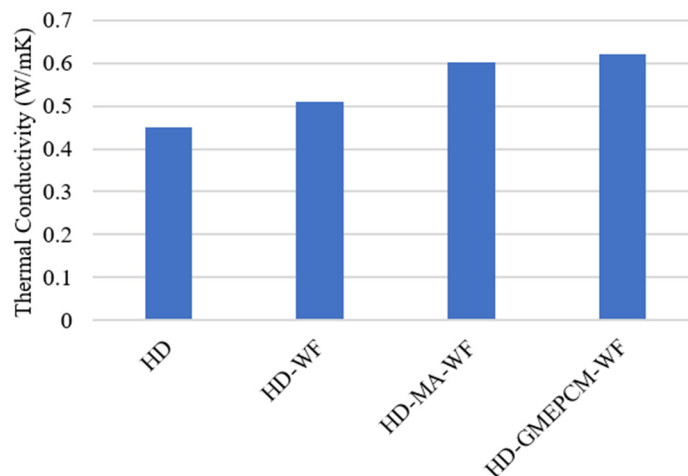
Fig. 13 Thermal conductivity of the materials

3.9 Thermal storage test

The results of the thermal storage test were revealed in Fig. 14. In this experiment, the temperature of samples was initially kept at -10.0 °C, and then exposed to light, and the surface temperature of the samples was for 15 minutes. It is traceable that the temperature of the HD-GMEPCM-WF composite rises slowly, which proves that it has the characteristics of thermal storage and the function of regulating temperature. The maximum temperatures of HD-WF and HD-GMEPCM-WF are 25.1 and 22.6 °C, respectively. It is widely acknowledged that every 1 °C increase in air conditioner temperature can result in a 6% reduction in electricity consumption. Therefore, the addition of GMEPCM is expected to save approximately 15% in electricity

consumption. As this composite material is applied to the inner construction materials, it will lower the room temperature and reduce the usage of the air conditioner. Furthermore, it will reduce carbon emissions, electricity usage, and the exacerbation of global warming.
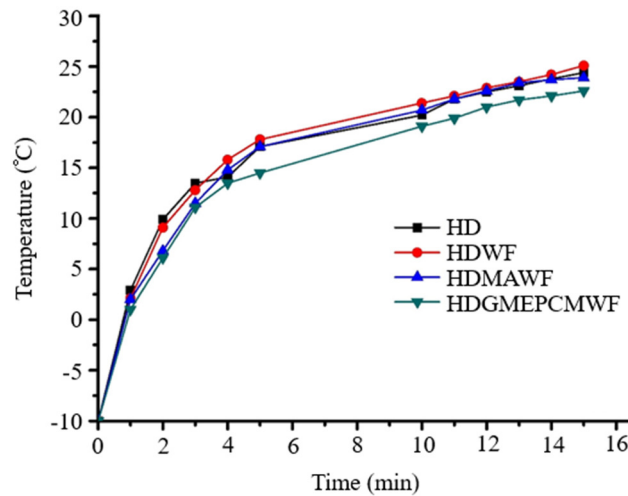
Fig. 14 Thermal storage test

4. Conclusions

In this study, nano-graphite-containing phase change microcapsules with good thermal conductivity and thermal storage capacity were successfully prepared. Moreover, the microcapsules were incorporated into HDPE to form a temperature-regulating building material.

(1) In the FTIR analysis, the results showed that the copolymer has been successfully synthesized and PCM has been successfully encapsulated in the shell.

(2) The results also showed that the encapsulation efficiency of PCM was increased, and the crystallization rate of PCM became faster when the NGP was added. Such results can be attributed to the significance of fine particles of NGP to the nucleating agent and the high thermal conductivity of the NGP, promoting the crystallization of octadecane.

(3) In the tensile test, the results showed that the compatibilizer is indispensable to the increase of interfacial adhesion of the WF and HDPE and the ensuing improvement of HDPE's tensile strength. However, the tensile strength was slightly reduced after adding microcapsules. The reason is that the unity aspect ratio of the microcapsules has no reinforcing effect on the tensile strength.

(4) The results also showed that the thermal conductivity of HDPE increased from 0.45 W/m·K to 0.62 W/m·K after the addition of GMEPCM. The thermal storage test showed that the HD-GMEPCM-WF composite material has the characteristics of thermal storage and the function of regulating temperature. Hence, it has great application prospects in building composite materials (such as flooring, partition walls, wall surfaces, etc.) to save electricity usage, reduce carbon emissions, and slow down global warming.

Conflicts of Interest

The authors declare no conflict of interest.

References

[1] W. Xu, Y. Wang, H. Xing, J. Peng, and Y. Luo, "Optimization of UiO-66/CaCl2 Composite Material for Thermal Energy Storage," Microporous and Mesoporous Materials, vol. 355, article no. 112574, May 2023.

[2] R. Sathyamurthy, "Silver (Ag) Based Nanoparticles in Paraffin Wax as Thermal Energy Storage for Stepped Solar Still – An Experimental Approach," Solar Energy, vol. 262, article no. 111808, September 2023.

[3] J. Wang and Y. Huang, "Exploration of Steel Slag for Thermal Energy Storage and Enhancement by Na2CO3 Modification," Journal of Cleaner Production, vol. 395, article no. 136289, April 2023.

[4] N. James, A. Mahvi, and J. Woods, "Optimizing Phase Change Composite Thermal Energy Storage Using the Thermal Ragone Framework," Journal of Energy Storage, vol. 56, no. A, article no. 105875, December 2022.

[5] S. Kahwaji, M. B. Johnson, and M. A. White, "Thermal Property Determination for Phase Change Materials," The Journal of Chemical Thermodynamics, vol. 160, article no. 106439, September 2021.

[6] Y. Liu, N. Wang, and Y. Ding, "Preparation and Properties of Composite Phase Change Material Based on Solar Heat Storage System," Journal of Energy Storage, vol. 40, article no. 102805, August 2021.

[7] V. Soni, "Nanoadditive Particles Segregation and Mobility in Phase Change Materials," International Journal of Heat and Mass Transfer, vol. 165, no. A, article no. 120676, February 2021.

[8] C. Li, X. Zhao, and J. Chen, "Diversiform Microstructure Silicon Carbides Stabilized Stearic Acid as Composite Phase Change Materials," Solar Energy, vol. 201, pp. 92-101, May 2020.

[9] Y. Liu and J. Jiang, "Preparation of β-Ionone Microcapsules by Gelatin/Pectin Complex Coacervation," Carbohydrate Polymers, vol. 312, article no. 120839, July 2023.

[10] J. Liang, X. Zhang, and J. Ji, "Hygroscopic Phase Change Composite Material——A Review," Journal of Energy Storage, vol. 36, article no. 102395, April 2021.

[11] H. Wang, E. Ci, X. Li, and J. Li, "The Magnesium Nitrate Hexahydrate with Ti4O7 Composite Phase Change Material for Photo-Thermal Conversion and Storage," Solar Energy, vol. 230, pp. 462-469, December 2021.

[12] L. Lv, J. Wang, M. Ji, Y. Zhang, S. Huang, K. Cen, et al., "Effect of Structural Characteristics and Surface Functional Groups of Biochar on Thermal Properties of Different Organic Phase Change Materials: Dominant Encapsulation Mechanisms," Renewable Energy, vol. 195, pp. 1238-1252, August 2022.

[13] Y. F. Shih, Z. T. Liao, N. C. Tsai, and Y. H. Chen, "The Application of Magnesium Nitrate Hexahydrate/Hybrid Carbon Material Phase Change Composites in Solar Thermal Storage," Journal of the Chinese Chemical Society, vol. 70, no. 8, pp. 1644-1655, August 2023.

[14] W. Liang, Y. Wu, H. Sun, Z. Zhu, P. Chen, B. Yang, et al., "Halloysite Clay Nanotubes Based Phase Change Material Composites with Excellent Thermal Stability for Energy Saving and Storage," RSC Advances, vol. 6, no. 24, pp. 19669-19675, February 2016.

[15] Q. Al-Yasiri and M. Szabó, "Incorporation of Phase Change Materials into Building Envelope for Thermal Comfort and Energy Saving: A Comprehensive Analysis," Journal of Building Engineering, vol. 36, article no. 102122, April 2021.

[16] Y. Chang and Z. Sun, "Synthesis and Thermal Properties of n-Tetradecane Phase Change Microcapsules for Cold Storage," Journal of Energy Storage, vol. 52, no. B, article no. 104959, August 2022.

[17] S. Qin, H. Li, and C. Hu, "Thermal Properties and Morphology of Chitosan/Gelatin Composite Shell Microcapsule via Multi-Emulsion," Materials Letters, vol. 291, article no. 129475, May 2021.

[18] Y. Konuklu and H. Akar, "Promising Palmitic Acid/Poly(Allyl Methacrylate) Microcapsules for Thermal Management Applications," Energy, vol. 262, no. B, article no. 125491, January 2023.

[19] K. S. Reddy, V. Mudgal, and T. K. Mallick, "Review of Latent Heat Thermal Energy Storage for Improved Material Stability and Effective Load Management," Journal of Energy Storage, vol. 15, pp. 205-227, February 2018.

[20] G. Alva, Y. Lin, L. Liu, and G. Fang, "Synthesis, Characterization and Applications of Microencapsulated Phase Change Materials in Thermal Energy Storage: A Review," Energy and Buildings, vol. 144, pp. 276-294, June 2017.

[21] J. Fukai, M. Kanou, Y. Kodama, and O. Miyatake, "Thermal Conductivity Enhancement of Energy Storage Media Using Carbon Fibers," Energy Conversion and Management, vol. 41, no. 14, pp. 1543-1556, September 2000.

[22] Y. Cui, C. Liu, S. Hu, and X. Yu, "The Experimental Exploration of Carbon Nanofiber and Carbon Nanotube Additives on Thermal Behavior of Phase Change Materials," Solar Energy Materials and Solar Cells, vol. 95, no. 4, pp. 1208-1212, April 2011.

[23] J. Xiang and L. T. Drzal, "Investigation of Exfoliated Graphite Nanoplatelets (xGnP) in Improving Thermal Conductivity of Paraffin Wax-Based Phase Change Material," Solar Energy Materials and Solar Cells, vol. 95, no. 7, pp. 1811-1818, July 2011.

[24] R. Al-Shannaq, J. Kurdi, S. Al-Muhtaseb, and M. Farid, "Innovative Method of Metal Coating of Microcapsules Containing Phase Change Materials," Solar Energy, vol. 129, pp. 54-64, May 2016.

[25] D. Q. Ng, Y. L. Tseng, Y. F. Shih, H. Y. Lian, and Y. H. Yu, "Synthesis of Novel Phase Change Material Microcapsule and Its Application," Polymer, vol. 133, pp. 250-262, December 2017.

[26] H. L. Chen, H. R. Shih, S. Wu, and Y. S. Chang, "Effects of Bi3+ Ion-Doped on the Microstructure and Photoluminescence of La0.97Pr0.03VO4 Phosphor," Advances in Technology Innovation, vol. 6, no. 3, pp. 191-198, July 2021.

[27] J. Sun, J. Zhao, B. Wang, Y. Li, W. Zhang, J. Zhou, et al., "Biodegradable Wood Plastic Composites with Phase Change Microcapsules of Honeycomb-BN-Layer for Photothermal Energy Conversion and Storage," Chemical Engineering Journal, vol. 448, article no. 137218, November 2022.